

AD-A119 742

TEXAS UNIV AT AUSTIN DEPT OF CHEMISTRY

F/6 7/4

INFRARED STUDIES OF CO ADSORPTION ON REDUCED AND OXIDIZED PT/TI--ETC(U)

AUG 82 K TANAKA, J M WHITE

N00014-75-C-0922

UNCLASSIFIED

TR-27

NL



END
DATE
FILMED
11 82
DTIC

12

AD A119742

OFFICE OF NAVAL RESEARCH

Contract N00014-75-C-0922

Task No. NR 056-578

TECHNICAL REPORT NO. 27

Infrared Studies of CO Adsorption on

Reduced and ~~Matinized~~ Pt/TiO₂

by

Katsumi Tanaka and J. M. White

Prepared for publication

in

Journal of Catalysis

Department of Chemistry

University of Texas at Austin

Austin, Texas 78712

August 17, 1982

Reproduction in whole or in part is permitted for
any purpose of the United States Government.

This document has been approved for public release
and sale; its distribution is unlimited.

DTIC
SELECTED
SEP 29 1982
S D H

DTIC FILE COPY

82 09 29 008

REPORT DOCUMENTATION PAGE		READ INSTRUCTIONS BEFORE COMPLETING FORM
1. REPORT NUMBER	2. GOVT ACCESSION NO. AD-A119742	3. RECIPIENT'S CATALOG NUMBER
4. TITLE (and Subtitle) Infrared Studies of CO Adsorption on Reduced and Oxidized Pt/TiO ₂		5. TYPE OF REPORT & PERIOD COVERED Technical Report 27 Jan. 1 - Dec. 31, 1982
7. AUTHOR(s) Katsumi Tanaka and J. M. White		6. PERFORMING ORG. REPORT NUMBER
9. PERFORMING ORGANIZATION NAME AND ADDRESS J. M. White Dept. of Chemistry, University of Texas Austin, TX 78712		8. CONTRACT OR GRANT NUMBER(s) N00013-75-C-0922
11. CONTROLLING OFFICE NAME AND ADDRESS Department of the Navy Office of Naval Research Arlington, VA 22217		10. PROGRAM ELEMENT, PROJECT, TASK AREA & WORK UNIT NUMBERS Project NR-056-578
14. MONITORING AGENCY NAME & ADDRESS (if different from Controlling Office)		12. REPORT DATE August 17, 1982
		13. NUMBER OF PAGES 38
		15. SECURITY CLASS. (of this report)
		16. DECLASSIFICATION/DOWNGRADING SCHEDULE
18. DISTRIBUTION STATEMENT (of this Report) Approved for public release: distribution unlimited.		
17. DISTRIBUTION STATEMENT (of the abstract entered in Block 20, if different from Report)		
19. SUPPLEMENTARY NOTES Prepared for publication in Journal of Catalysis; preprint, accepted		
20. KEY WORDS (Continue on reverse side if necessary and identify by block number) 1854 cm ⁻¹ / 2094 cm ⁻¹		
21. ABSTRACT (Continue on reverse side if necessary and identify by block number) Carbon monoxide adsorption experiments were studied on reduced and oxidized Pt/TiO ₂ with FT-IR. On reduced samples two kinds of linear CO species were observed and assigned as adsorption on Pt close-packed (terrace) sites (2094 cm ⁻¹). In addition a bridged CO species was found at 1854 cm ⁻¹ . Both linear species show increasing frequencies with coverage. Saturation CO uptake decreases with increasing substrate reduction temperature and there is a preferential decrease of linear CO CO species on terrace sites and the		

DD FORM 1473

1 JAN 73

EDITION OF 1 NOV 65 IS OBSOLETE
S/N 0102-010-0001

SECURITY CLASSIFICATION OF THIS PAGE (When Data Entered)

Block 20. Continued.

concentration of bridged species lies below detection limits. On oxidized Pt/TiO₂ samples, some Pt atoms are covered with oxygen atoms and the density of step sites is enhanced. On these surfaces there are two kinds of linear CO species assigned to terraces (2130 cm⁻¹) and steps (2101 cm⁻¹) and a bridged CO species at 1880 cm⁻¹. In addition, several CO species are also detected on reduced samples. These species show intensity variations during lengthy exposures. Preadsorbed linear CO species (2130 cm⁻¹, 2094 cm⁻¹ and 2077 cm⁻¹ bands) on oxidized samples are also sensitive to H₂ exposures.

(104) final

Sept 6-13-82

Infrared Studies of CO Adsorption on Reduced and Oxidized Pt/TiO₂

Katsuni Tanaka and J. N. Whitcomb
Department of Chemistry
University of Texas
Austin, Texas 78713

supported in part by the Office of Naval Research.
Requests for correspondence should be addressed.

Abstract

Carbon monoxide adsorption experiments were studied on reduced and oxidized Pt/TiO₂ with FT-IR. On reduced samples two kinds of linear CO species were observed and assigned as adsorption on Pt close-packed (terrace) sites (2094 cm⁻¹) and on Pt open (step) sites (2077 cm⁻¹). In addition a bridged CO species was found at 1854 cm⁻¹. Both linear species show increasing frequencies with coverage. Saturation CO uptake decreases with increasing substrate reduction temperature and there is a preferential decrease of linear CO species on terrace sites and the concentration of bridged species lies below detection limits. On oxidized Pt/TiO₂ samples, some Pt atoms are covered with oxygen atoms and the density of step sites is enhanced. On these surfaces there are two kinds of linear CO species assigned to terraces (2130 cm⁻¹) and steps (2101 cm⁻¹) and a bridged CO species at 1880 cm⁻¹. In addition, several CO species are found which are also detected on reduced samples. These species show intensity variations during lengthy exposures. Predominant linear CO species (2130 cm⁻¹, 2094 cm⁻¹ and 2077 cm⁻¹ bands) on oxidized samples are also sensitive to H₂ exposures.

Accession For		DTIC GRAFI		Unannounced		Distribution/		Availability Codes		Avail and/or		Dist	
												A	
												Special	

DTIC
COPY
UNCLASSIFIED

1. Introduction

The absorption of CO is typically used in the characterization of supported metal catalysts. Since Elshens et al reported observed CO species on γ - Al_2O_3 and SiO_2 supported Pd, Ni and Pt catalysts, (1) much attention has been given to the type of CO, i.e. linear, bridged and twin species. (2) In general it is found that the CO absorption depends on the metals themselves, their dispersion and oxidation state, as well as the support. Taking Pt catalysts for example, linear and bridged CO species are observed at 2040-2100 cm^{-1} and 1818-1865 cm^{-1} irrespective of their supported or non-supported character; i.e., on Pt/ γ - Al_2O_3 , (1,3) evaporated Pt films, (4) Pt(111) (5) and Pt/Ti-silites. (6) An exception is the Pt/ SiO_2 system where only a linear CO species is seen. (1) Hupkes and Ibach performed IR and LMD measurements on Pt(111) and Pt 6(111)x(111) systems and observed linear CO species at 2009 cm^{-1} when the LMD pattern shows the $\sqrt{3}\times\sqrt{3}$ R30 structure while bridged species at 1895 cm^{-1} were involved in the C(au2) structure. (7)

It is reported that Pt supported on high temperature pretreated TiO_2 shows a high catalytic activity for the photo-assisted water decomposition and water gas shift reactions. (8) TiO_2 -supported metal catalysts also show striking CO and H_2 uptake decreases with increasing reduction temperature, called the strong metal support interaction (SMSI), (9) and high catalytic activity and selectivity are reported for such systems. (10)

The aim of this paper is to characterize the CO adsorption sites both on oxidized and reduced Pt/ TiO_2 . Coadsorption experiments using C^{16}O and C^{18}O (11) and C^{18}O exchange reaction (12) predicted species were performed on reduced catalysts in support of this characterization. In addition CO adsorption on oxidized-Pt/ TiO_2 and the subsequent effect of H_2 introduction was examined.

2. Experimental

A commercial anisole sample (NCS) was used as the support after overnight reduction with H_2 at 800°C. This is the same procedure used to obtain high activity for the photoassisted water decomposition reaction. (8) The main impurities in the sample were As(0.00028), Fe(0.0108), Pb(0.0028) and Zn(0.018). Reduced TiO_2 was soaked in dilute chloroplatinic acid solution to prepare 2 wt% Pt loaded catalysts. This solution was dried at 100°C and the supported catalyst was washed with distilled water at 25°C until no chlorine was detected in solution. Carbon monoxide was purified through a 5A molecular sieve trap maintained at 77K.

An infrared cell, with CaF_2 windows, was designed to prepare the sample in situ. (11) Infrared spectra were recorded in absorbance using a Nicolet 7199 Fourier transform infrared spectrometer with 2 cm^{-1} resolution. Three hundred scans were taken to get good S/N. Absorption due to the windows and the gas phase were subtracted. CO was introduced to each sample at 25°C and infrared spectra were recorded at the same temperature.

Pellets for infrared experiments were prepared between pieces of paraffin paper moistened, using stopcock grease, to the faces of

a one inch diameter die. A pressure of 5000 lb in⁻² was applied to 130 mg in⁻² of powder. Without paraffin paper, attempts to prepare pellets were unsuccessful. There are advantages and disadvantages in this procedure. Metal contamination from the pellet die is minimal and sturdy infrared pellets are formed. However, pellets show paraffin adsorption bands which must be removed by oxidation at 400°C overnight. While we cannot rule out subtle changes in substrate structure as a result of this procedure no qualitative difference was observed for CO adsorption on Pt supported on unreduced anatase and the pretreated, reoxidized TiO₂ described above.

Carbon monoxide adsorption experiments were carried out on three kinds of samples: oxidized, reduced at 200°C and reduced at 400°C. In each case the final step was evacuation at 400°C for 30 minutes. The three types are denoted as 400-40-400, 400-200-400 and 400-400-400, where each number shows the treatment temperature in the following order: oxidation, reduction with H₂ and evacuation. Oxidation and reduction treatments were done in a static system. During reduction, 1 atm of purified hydrogen was replaced at least 5 times. The quantitative analysis of CO uptake gave CO/Pt=0.20 on Pt/TiO₂ (400-200-400).

3. Results and Discussion

In the sections below several CO stretching frequencies are assigned. These are summarized in Table 1, and the assignments of each band are summarized in Table 2.

3.1. CO adsorption on Pt/TiO₂ (400-200-400)

CO adsorption spectra on Pt/TiO₂ reduced at 200°C with H₂

overnight and subsequently evacuated at 400°C (400-200-400) are shown in Fig. 1. Introduction of 5 torr CO, Fig. 1(a), showed infrared absorption bands at 2185 cm⁻¹, 2092 cm⁻¹ and 1854 cm⁻¹. The 2092 cm⁻¹ and 1854 cm⁻¹ bands can be assigned to linear and bridged CO on Pt respectively in agreement with the early work of Eickens and Pliskin.⁽¹⁾ The 2185 cm⁻¹ band was observed in CO adsorption on TiO₂ and was assigned as a physisorbed species,⁽¹¹⁾ however, the gas phase CO frequency is 2143 cm⁻¹ so that it may be better to assign 2185 cm⁻¹ as a weakly chemisorbed species. Upon evacuation at 25°C, Fig. 1(e) is converted to Fig. 1(b); the 2185 cm⁻¹ band disappears, the linear Pt-CO species shifts down to 2078 cm⁻¹ and the bridged CO remains at 1854 cm⁻¹ but with lower intensity. This is quite different from the behavior on alumina-supported Pt catalysts, where the bridged species is easily removed during evacuation at 25°C.^(3a) Spectrum 1(c), after evacuation at 80°C, showed no bridged species and an adsorption maximum at 2063 cm⁻¹ with a shoulder at 2074 cm⁻¹. After 150°C evacuation this shoulder disappeared leaving a single peak at 2060 cm⁻¹, Fig. 1(d). No CO remained after evacuation at 200°C, Fig. 1(e). In order to check the reproducibility, 5 torr CO was introduced after experiment 1(e). As shown, Fig. 1(f) reproduces Fig. 1(a) except the shoulder at 2082 cm⁻¹ is resolved and there is a 20% decrease in intensity.

The downward frequency shift of linear CO frequency with decreasing CO coverage is a common observation. One of the earliest observations was for CO on Pt/TiO₂ where the shift was from 2087 to 2040 cm⁻¹, a shift attributed to dipole-dipole

interactions. (12) However, Rytov (13) proposed that the formation of a strong bond enhances back donation from metal d-orbitals to antibonding $2\pi^*$ orbital of the CO molecule, thereby weakening the C-O bond. This would cause the frequency to shift downward. Since the metal-CO bond energy typically decreases with coverage, we would expect the stretching frequency to decrease as the coverage decreases. As Hollins and Pritchard (14) suggest, this idea of explanation is chemical in nature and has a quite different origin than the dipole-dipole interactions.

Infrared-absorption spectra for CO on polycrystalline Pt, described by the (111) face, show a frequency shift from 2055 to 2101 cm^{-1} as the coverage increases to saturation (15). Crowley and King (15) use a model, first developed by Sumner et al. (12) to account for this frequency shift. It involves experimental vibrational spectra, from isotopic mixtures of ^{13}CO and ^{12}CO . If the shift of the ^{12}CO band to higher frequency with increasing coverage is due only to dipole-dipole interactions, then successive substitution of ^{13}CO with ^{12}CO , at constant total coverage so the metal-CO interaction is constant, should reduce the frequency. They obtained this result experimentally. The essential feature of the model is the frequency shift, which is proportional to the lattice sum, $\sum_{ij} R_{ij}^{-3}$, where R_{ij} is the distance between the centers of two dipoles i and j. Similar coverage induced frequency shifts have been reported for Pt (16) and Cu (17) surfaces. For Pt, frequency shifts are also observed for bridged CO on Pt (17) and Pt₂ (18).

To test whether or not the shift shown in Fig. 1 was due to dipole-dipole interactions, equimolar C^{16}O and C^{18}O (6 torr) was introduced on Pt/ TiO_2 (400-200-400). As shown in Fig. 2(a), linear C^{16}O and C^{18}O species on Pt were observed at 2074 cm^{-1} and at 2007 cm^{-1} . On TiO_2 , C^{16}O and C^{18}O gave bands at 2105 cm^{-1} and 2135 cm^{-1} . Isotopically different bridged species were not resolved here; however, bridged C^{16}O and C^{18}O species were resolved at 1954 cm^{-1} and 1910 cm^{-1} using a different procedure (Fig. 3). After evacuation at 25°C, the 2074 cm^{-1} band shifted to 2061 cm^{-1} , while the relative intensity of the shoulder at 2007 cm^{-1} grew with no frequency shift. These two bands shifted to lower frequency with lower CO coverage as the evacuation temperature was increased to 80°C (Fig. 2(c), and to 150°C, Fig. 2(d). Evacuation at 200°C, Fig. 2(e), left no detectable adsorbed CO. Comparing 1a with 2a and 1b with 2b, we note that under similar coverage conditions the C^{16}O stretching frequency is always reduced in the presence of C^{18}O .

Etchens, et al. (1) observed two bands at 2074 cm^{-1} and 2012 cm^{-1} when a mixture of ^{12}CO and ^{13}CO was adsorbed on a Pt/ SiO_2 catalyst. (Note that the isotope effect of $^{13}\text{CO}/^{12}\text{CO}$ is almost the same as $\text{C}^{18}\text{O}/\text{C}^{16}\text{O}$ so results can be compared directly.) They find that chemisorbed CO is pumped out at 200°C and that the relative intensities of the two bands depends on the surface coverage with the high frequency band becoming relatively more intense as the surface coverage increases, just as we observe in Fig. 2. This is interpreted in terms of dipole coupling variations.

Our results are quite consistent with theirs. We conclude that for CO on Pt/TiO₂ (400-200-400) the 2092 cm⁻¹ band is a linear species and the frequency shift of this species can be interpreted completely in terms of dipole-dipole interactions between adsorbed species.

The exchange of C¹⁸O with C¹⁶O preadsorbed on Pt/TiO₂ at 25°C was used as a complement to the adsorption experiment described above. First 3 torr of C¹⁶O was dosed onto a 400-200-400 Pt/TiO₂ sample, Fig. 3(a), and followed by evacuation at 25°C, Fig. 3(b). When this surface was exposed to 3 torr C¹⁸O, the linear C¹⁶O species on Pt changed to the C¹⁸O homologue at 2042 cm⁻¹, with a shoulder at 2077 cm⁻¹, and bridged C¹⁶O at 1854 cm⁻¹ changed quickly (5 min.) to bridged C¹⁸O at 1816 cm⁻¹, Fig. 3(c). The shoulder at 2077 cm⁻¹ gradually decreased in intensity with time of exposure to C¹⁸O, Fig. 3(d) is after 30 min. and Fig. 3(e) is after 18 hr. During this same period the bridged CO species moved to 1816 cm⁻¹. The isotopic frequency ratios of the 1816 cm⁻¹/1854 cm⁻¹ and 2042 cm⁻¹/2094 cm⁻¹ bands are consistent with the theoretical value (0.9739).

Evacuation at 25°C, Fig. 3(f), had little effect on the spectrum but upon evacuation at 80°C, two bands were observed at 2092 cm⁻¹ and 2009 cm⁻¹, Fig. 3(g). It is very interesting to compare this with Fig. 2(c) which was recorded after evacuation at the same temperature following a 1:1, C¹⁶O:C¹⁸O, adsorption experiment. About 90% of all the adsorbed C¹⁶O on Pt exchanges readily with C¹⁸O. The remaining 10% is associated with the C¹⁶O species at 2009 cm⁻¹, Fig. 3(h), and does not exchange readily.

This C¹⁶O species is adsorbed strongly and remains, with a frequency shift to 2050 cm⁻¹, after evacuation at 80°C, Fig. 3(i). The equilibration of isotopic species in the exchange is heavily weighted in favor of adsorbed C¹⁸O because of the dominance (50/1) of C¹⁸O in the gas phase. These results imply that adsorbed C¹⁶O species which rapidly exchange with gas phase C¹⁸O at 25°C are those species removed by evacuation at 80°C. Moreover, the evidence suggests that the CO species at 2050 cm⁻¹ remaining after evacuation at 150°C, Fig. 1(d), and after the exchange reaction with C¹⁸O, Fig. 3(c), (g), is not the same species as that showing a strong band at 2094 cm⁻¹, Figs. 1(a), 3(a). We propose that the 2094 cm⁻¹ band is due to CO on terrace sites while the band at 2050 cm⁻¹ involves step site adsorption. In the following paragraphs we relate this idea to observations on unsupported metals.

According to X-ray diffraction results for the Pt/TiO₂ system, the surface of supported Pt is composed mainly of (111) faces with a small amount of the (200) face (9a,19). It is also well known that the (111) face is dominant for stepped polycrystalline Pt. (20) Therefore it is worthwhile considering CO adsorption experiments done on Pt(111). Several studies (21-23) of CO adsorption on Pt(111) indicate that the activation energy for desorption drops monotonically with CO coverage and that the activation energy for desorption, extrapolated to zero coverage, is about 13 kcal mole⁻¹. In these experiments there is no evidence for the different kinds of species and sites that would account for the distinctly different isotopic exchange rates that

3.2 CO adsorption on Pt/TiO₂ (400-400-400)

Adsorption of CO was carried out on Pt/TiO₂ after overnight oxidation followed by reduction and evacuation, all at 400°C (Fig. 4). We selected 400°C as the maximum hydrogen/reduction temperature (which gives a mild SMSI system) because a complete SMSI system (reduced at 500°C) is known to reduce the CO uptake at 25°C by as much as a factor of 20. (9,19) Under these conditions, CO bands are difficult to detect. In an ambient of 10 torr CO, Fig. 4(a), infrared absorption was recorded at 2185 cm⁻¹ and 2083 cm⁻¹ which correspond to CO on TiO₂ and linear CO on Pt, respectively. It is noteworthy that the intensity of the CO species on Pt decreased by about 50% relative to the spectrum of Fig. 1(a). Moreover, no bridged CO species was seen. This is not merely a signal-to-noise problem since a 50% reduction of the 1854 cm⁻¹ band of Fig. 1(a) would still be easily measured. As shown in Fig. 4(b), the linear CO species on Pt at 2083 cm⁻¹ shifted to 2072 cm⁻¹ upon evacuation at 25°C for 30 min. Following this procedure, 1 atm CO was added, Fig. 4(c). Approximately the same intensity CO band as observed in Fig. 4(a) was seen at 2081 cm⁻¹ with some complicated bands at around 2170 cm⁻¹. Evacuation at 25°C and 150°C, Fig. 4(d), 4(e), caused a frequency shift of linear CO species on Pt from 2081 to 2075 cm⁻¹ and 2065 cm⁻¹ with accompanying losses of intensity. In Fig. 4(f) two small intensity bands were detected around 1940 and 1840 cm⁻¹. These are not associated with CO since they often appear on reduced samples in the absence of CO. Although the origin of these bands

is obscure.

Stepped or kinked Pt(111) does show site heterogeneity in CO desorption; two peaks appear (7,24-26), and the intensity ratio follows the step/terrace concentration ratio. While there are significant variations in the quoted activation energies for desorption, there is agreement that desorption from step sites involves at least 3 kcal mole⁻¹ higher activation energy than desorption from the terrace sites. Consequently, it is not unreasonable to expect some variations in isotopic molecular exchange rates. If CO adsorbed at step (and other defect) sites exchanges slowly, compared to CO adsorbed at terrace sites, then we would expect this to be reflected in experiments like those summarized in Fig. 3. Thus we interpret the 2050 cm⁻¹ band in Fig. 3(g) as C¹⁸O adsorbed on step sites. Note the similarity between Fig. 2(d) and Fig. 3(g).

Because connections to single crystal work involving the step/terrace concepts are made here we have chosen to use this language. It should be recognized that one could also use the language of closed-packed (111) and open (higher index) crystallite faces.

Recently Bertok et al. (27) found adsorption-desorption hysteresis curves in CO on Pt supported cub-o-o-ell systems, where high frequency "adsorptive CO" is ascribed to disordered species while low frequency "desorptive CO" is ascribed to ordered species. According to their results, CO molecules migrate from low Miller index planes, terraces, to high Miller planes, steps and kinks, prior to desorption. Their observations with respect to surface heterogeneity are consistent with our results.

is unknown, they may be associated with overtones of Ti-O lattice vibrations. The 2065 cm^{-1} band remained following evacuation at 200°C , Fig. 4(f). This is quite different from the behavior shown by Pt/TiO_2 reduced at only 200°C , Figs. 1-3, where all the CO bands disappear after evacuation at 200°C .

After the spectrum of Fig. 4(f) was taken, the sample was exposed to 6 torr of CO in order to check reproducibility. As indicated in Fig. 4(g), the frequency of CO on Pt shifted to 2075 cm^{-1} as compared to 2063 cm^{-1} in Fig. 4(a). Moreover, the intensity decreased about 50%. Evacuation at 25°C led to the expected decreased frequency shift, Fig. 4(h). Taking difference spectra (not shown), i.e. 4(b) - 4(a) and 4(h) - 4(g), clearly indicates that those species giving the 2060 cm^{-1} band partially rearranged and partially desorbed with evacuation to give the bands in the $2065 - 2071\text{ cm}^{-1}$ range. This suggests that either: (1) a CO molecule on a terrace migrates and is stabilized on a step or defect site or (2) that CO molecules adsorb primarily on step sites and, upon evacuation, the frequency of this band moves down due to lower dipole-dipole interactions. We favor the former explanation.

The uptake of both H_2 and CO on TiO_2 supported noble metal catalysts is strongly diminished by H_2 reduction at 500°C . This is not the result of metal agglomeration on the TiO_2 support since more than 2/3 of the original CO and H_2 uptake are recovered by reoxidation at 400°C . This observation is in contrast to the strong metal-support interaction (MSI) and has been shown to give significant effects in CO hydrogenation activity and

selectivity. (10)

The morphology of the Pt particles is significant. Baker, et al. (26) conclude from transmission electron microscopy that Pt on TiO_2 (in the SMI state) is in the form of thin hexagonal platelets grown over a partially reduced titania, Ti_2O_3 . The faces of these thin structures have Pt(111) character with mainly terrace sites. It is this structure which shows only weak CO chemisorption. Our results then suggest that a selective decrease in CO binding on terrace sites, perhaps due to changes in the Pt electronic structure, leads to the loss of CO chemisorption activity.

From IRPD and high resolution electron energy loss spectroscopy (HREELS) data, there are two ordered structures showing different CO binding on Pt(111).⁽⁷⁾ For the $\sqrt{3} \times \sqrt{3} \text{ R}30^\circ$ structure, only linear bonding is found while for the $c(4 \times 2)$ structure, both the linear (2069 cm^{-1}) and bridged (1855 cm^{-1}) structures are found. On a stepped surface, $6(111) \times (111)$, a linear species at 2069 cm^{-1} is also found even when the thermal desorption spectra clearly indicate that CO is bound only to step sites. The relatively low resolution of HREELS ($\sim 400\text{ cm}^{-1}$) may have prevented observation of shifts due to binding differences on terraces and steps.⁽²⁹⁾ These results are not inconsistent with the notion that, in the SMI system, terrace sites become dominant, that no bridge bonded CO is present on step sites and that linear CO binding on residual steps is still strong.

3.3 CO adsorption on Pt/TiO_2 (400-500-600)

Adsorption of CO on Pt/TiO_2 that was oxidized at 400°C and

around at 400°C (400-450-480) proved very interesting because various absorption bands changed position and intensity during the time of the experiment. Figure 5(a) shows that when an oxidized Pt/TiO_2 was exposed to 0.5 torr CO at 25°C , bands were observed at 2000 (CO on TiO_2), 2045 (CO on TiO_2), 2130 and 2094 (linear CO on Pt) and 2045 cm^{-1} (adsorbed CO on Pt). With exposure time, Fig. 5(b) and 5(c), the intensity of the 2130, 2045 and 1954 cm^{-1} bands steadily increased. The formation of a small new band was observed at 1905 cm^{-1} after 120 min. Fig. 5(d). In the early stages of the experiment, unknown carbonyls and isocyanides were observed. Bands appeared at 1905 and 2038 cm^{-1} .

After a total exposure to 0.5 torr CO, the CO pressure was reduced to 25 torr. The spectrum after 5 min, Fig. 5(e), showed that the intensity of the 2000 cm^{-1} band decreased steadily while the 2045 cm^{-1} band (assumed CO_2 on TiO_2) increased. At 10 minutes exposure, the 2045 cm^{-1} band was detected. In addition, several new bands for carbonyls of Fig. 5(f). With the 20-45 torr CO, a strong band appeared at 2000 cm^{-1} and was the dominant feature of the spectrum after 45 min, Fig. 5(g). During the 45-120 min, the 2000 cm^{-1} band disappeared, a relatively intense band appeared at 2000 cm^{-1} , the 2130 cm^{-1} band shifted to 2135 cm^{-1} , a band appeared at 1942 cm^{-1} and the band at 1905 cm^{-1} again increased significantly. Note that the carbonyls in the 45-120 min region that of the other carbonyls in Fig. 5.

Figure 5 shows the time dependence of the formation of the 2000 cm^{-1} band. It is interesting that the 2000 cm^{-1} band in

sensitive to the CO pressure and the 2130 cm^{-1} band goes through a maximum and then decreases (compare 4.5 and 67 hr in Fig. 6). Other experiments show that the formation rate of the 2000 cm^{-1} band depends both on the CO pressure and the relative amount of the 2130 cm^{-1} band. The spectral changes shown in Figs. 5 and 6 were reproducible after a reduction-oxidation cycle of the Pt/TiO_2 .

Spectra (h) through (n) of Fig. 5 characterize the thermal stability of the $\text{CO}/\text{Pt}/\text{TiO}_2$ system at Fig. 5(h) after evacuation at temperatures between 25 and 200°C . Upon evacuation at 25°C , Fig. 5(i), the intensity of the 2130, 2045, 1942 and 1904 cm^{-1} bands all decreased. Spectrum (j), obtained after evacuation at 80°C , shows selective desorption of the 2077 cm^{-1} band and another bands at 1942 and 1954 cm^{-1} . In the region above 200°C , there was significant loss of intensity associated with a 2100 cm^{-1} band (see below) which allowed a small band at 2130 cm^{-1} to be observed clearly. Desorption at 100°C , Fig. 5(k), was accompanied by a 20-fold loss of 2094 cm^{-1} intensity with a shift of the 2077 cm^{-1} band to 2069 cm^{-1} with a 70% loss of intensity. Desorption at 200°C completely removed the observed carbonyls, Fig. 5(n).

After evacuation at 200°C , the sample was re-exposed to torr CO. Figure 5(l), taken after 5 min exposure to 0.5 torr CO, shows that the 2130 cm^{-1} band is a factor of 10 weaker relative to spectrum 5(i) and that the formation of the 2000 cm^{-1} band was much faster than shown in Figs. 5(a)-(g). This experiment is interpreted to mean that the surface of oxidized Pt/TiO_2 is

reduced with CO and the formation rate of the 2080 cm^{-1} intensity is inversely proportional to the intensity of the 2130 cm^{-1} band.

The results of a series of experiments, like those of Fig. 5, can be summarized as follows (see Table 1 for assignments):

(a) On a Pt/TiO_2 surface produced with O_2 at 400°C exposure to CO leads to bands associated with and without interacting oxygen. The former is found at 2130 cm^{-1} (Fig. 5a) and the latter at 2087 and 2077 cm^{-1} (Fig. 5b). The formation rate of the 2077 cm^{-1} band is dependent on the CO pressure.

(b) On the same surface there are two kinds of bridged CO (1880 and 1854 cm^{-1}). The intensities of the 1880 and 2130 cm^{-1} bands are related. These are assigned (see below) to CO adsorbed in bridged and linear forms that also involve chemisorbed oxygen.

(c) With exposure time, the 2130 cm^{-1} band reaches a maximum intensity and shifts to lower frequency. This species is ascribed to linear CO on Pt with interacting oxygen since the intensity decreased sharply following surface reduction.

(d) The intensity decrease with time of the physisorbed CO species on TiO_2 at 2185 cm^{-1} is associated with the formation of coordinated CO_2 at 2345 cm^{-1} , as well as some carbonate species, on TiO_2 .

In the previous sections we suggested two kinds of CO on Pt/TiO_2 , terrace and step $\text{Pt}(111)$ sites. This also appears to be the case for oxygen produced Pt/TiO_2 . Before considering the details, we briefly consider the interaction of O_2 with Pt. Molecule adsorbed, atomically chemisorbed and subsurface oxide are all known to exist in the $\text{O}_2/\text{Pt}(111)$ system.⁽³⁰⁾ In our

system molecular adsorption is negligible since the sample is evacuated at 400°C . We expect the oxygen to be predominately chemisorbed atomic species although, for small Pt particles on TiO_2 , subsurface oxygen may be formed. This remains an open question deserving further study. We attribute the 2130 cm^{-1} band to CO on Pt in the presence of atomic oxygen.

On well-characterized bulk single crystals, dissociation of O_2 on Pt takes place mainly on step sites, as compared to terrace sites.⁽²⁵⁾ Assuming, then, that oxygen atoms are chemisorbed primarily on step sites in our system, we expect selective CO adsorption on terrace sites (2094 cm^{-1}) until the oxygen atoms at the steps are removed. The CO pressure dependence of the 2080 cm^{-1} band (Fig. 6), which is assigned to CO on step sites, can be interpreted in terms of selective adsorption of oxygen atoms on these sites followed by a slow reaction with CO, removal as CO_2 and, finally, CO adsorption at the same sites.

In a supporting experiment, a (400-NO-400) sample was exposed to 1 atm of O_2 for 30 min at 25°C , evacuated at 25°C and exposed to 7 torr of CO at 25°C . Comparing Fig. 7(a) and (b) with Fig. 5(a) and (b), there are no qualitative differences suggesting that the adsorbed oxygen reactivity and structure does not depend on either the adsorption or evacuation temperature between 25 and 400°C . Figure 7(c) shows that the 2080 cm^{-1} band intensity grew in during evacuation at 25°C . We take this to mean that step sites were vacated during evacuation by reaction of CO with O(a) and removal as CO_2 , thereby allowing terrace CO to migrate to the step sites. Spectrum 7(d), seen after evacuation at 100°C , shows

that the 2130 cm^{-1} band is composed of two species with frequencies at 2130 and 2101 cm^{-1} .

The presence of two kinds of CO on oxygen covered Pt reminds us that there are two kinds of CO on reduced Pt, terrace and step species. If it is assumed that the 2130 and 2101 cm^{-1} bands correspond to terrace and step adsorption on oxygen-covered Pt, then the downward frequency shift of mixtures of these two species in Fig. 5 can be accounted for as the result of enrichment of the 2101 cm^{-1} band. This assignment is supported by another experimental result. In Fig. 6 there is a linear relationship between the absorbance of the 2094 and 2130 cm^{-1} bands during the first two hours of the exposure, where the frequency of the CO on oxygen covered Pt remains at 2130 cm^{-1} .

The remaining assignments involve the bands at 2060 and 1942 cm^{-1} . These may be assigned to dicarbonyl species. If present, such species should give a pair of bands (symmetric and asymmetric) as in $\text{Ir}(\text{CO})_2$ (16) and $\text{Rh}(\text{CO})_2$ (31). These species formed on Y-alumina are thought to be on partially oxidized isolated metal sites like Rh^+ . The formation of such species would require extensive coordinative unsaturation as expected at steps, kinks and other defects. McClellan et al. (26) suggest that for the Pt(321) surface made of rough steps which have a high density of kinks, 40% of the surface Pt atoms are coordinatively unsaturated. Such surface sites could account for the formation of dicarbonyl species.

The results of introducing H_2 to a Pt/TiO₂ surface, pretreated with CO and evacuated at 25°C , are shown in Fig. 8. Prior to the

introduction of H_2 , the intensity of the 2094 , 2077 and 2130 cm^{-1} bands were 0.144 , 0.033 and 0.028 , respectively. Adding H_2 gave rise to a rapid intensity increase in the 2094 cm^{-1} band and an abrupt decrease of the 2077 and 2130 cm^{-1} bands. With H_2 exposure time, Fig. 8 shows that the 2094 and 2077 cm^{-1} band intensities increase gradually, while the band at 2130 cm^{-1} decreased slowly. After a 2 hr exposure, the frequencies of these three bands shifted down to 2080 , 2062 and 2118 cm^{-1} . The combined intensity of the 2094 and 2077 cm^{-1} bands was 0.178 at the start and rose to 0.196 after 2 hr . This increase matches nicely the intensity lost (0.019) in the 2130 cm^{-1} band and indicates that CO molecules on oxygen covered Pt are converted to CO species on step and terrace sites on reduced Pt during H_2 exposure. The growth of the 1620 cm^{-1} band, indicating water formation, is consistent with the above frequency shifts in the sense that surface reduction is occurring. Cavanagh and Yates (32) as well as Apple and Dybowski (33) studied the effect of coadsorption of CO on the adsorption of H_2 on $\text{Rh}/\text{Al}_2\text{O}_3$ and Rh/TiO_2 and concluded that preadsorbed CO inhibits the adsorption of "spillover" hydrogen. Applied to our system, we expect no reduction of TiO_2 and interpret the water indicated in Fig. 8 as arising from reaction with oxygen on Pt (hydrogen titration).

Two of the more interesting results of the experiment described in Fig. 8 are the downward frequency shift with time of the CO species on both step and terrace sites and the abrupt intensity changes in some of the bands just after hydrogen introduction. Downward frequency shifts are also observed in

coadsorption of H_2O and CO. This is explained in terms of strengthened chemical bonds between Pt and C. Though there is no hydrogen adsorption data that compares the characteristics of terrace and step sites, our intensity redistribution data suggests that: (a) most CO molecules on Pt are mobile and (b) hydrogen adsorbs in a way that removes some CO from step sites. Since H_2 adsorption is not likely to induce CO desorption, we expect that CO molecules removed from step sites will migrate to terrace sites. This result implies that CO and H on step sites have different adsorption structures than their counterparts on terrace sites. The initial sticking coefficient for H_2 is reported to be 0.2 for clean Pt(111) and 0.4 for oxygen covered Pt(111); however, the saturation coverage for H(a) is nearly the same in both cases. (23) Taking this result over to our supported Pt system, hydrogen adsorption would occur more readily on step sites since oxygen atoms prefer to adsorb there.

4. Summary.

The IR data reported here show clearly that a variety of adsorbed CO species are observed on platinumized titania depending on the pretreatment of the adsorbate. The absorption bands are interpreted in terms of the traditional bridged and linear CO species. Here, we find two types of linear CO species which are assigned to adsorption on terrace (close-packed) and step (open) sites. Detectable frequency shifts in both are found in the presence of adsorbed oxygen. Exchange experiments involving $C^{18}O$ and $C^{16}O$ demonstrate that the species attributed to step sites exchange more slowly than those at the terrace sites.

This is confirmed by thermal desorption experiments showing that the higher frequency linear CO component (terrace site) is less stable. In the strongly reduced SMI state, Pt/TiO₂ adsorbs small amounts of CO, bridged CO is not detected and adsorption at terrace sites is lost preferentially. On oxidized Pt/TiO₂, several kinds of adsorbed CO form and intensities are time dependent reflecting oxygen removal by reaction with CO to form CO₂, particularly at step sites. Under some conditions, weak bands assigned to dicarbonyl are found. Finally, exposure of a CO-preduced sample to H_2 causes marked changes in the intensities of certain CO bands indicating surface reduction to form water and a redistribution of linearly bound CO between step and terrace sites.

References

1. a. R. P. Elchman, S. A. Francis and W. A. Pilatkin, *J. Phys. Chem.*, **60**(1956)194.
- b. R. P. Elchman and W. A. Pilatkin, *Adv. Catalysis*, **10**(1958)11.
2. R. Upo, *Catalysis Rev.*, **11**(1973)255.
3. a. J. B. Ford, *J. Catalysis*, **52**(1978)144.
- b. W. G. Rothchild and E. C. Yao, *J. Chem. Phys.*, **74**(1981)4286.
4. a. C. W. Garland, R. C. Lord and P. P. Troiano, *J. Phys. Chem.*, **69**(1965)1368.
- b. G. Blyholder and R. Sheets, *J. Phys. Chem.*, **74**(1970)4335.
5. a. K. A. Shigaishi and D. A. King, *Surface Sci.*, **58**(1976)379.
- b. A. Greenley and D. A. King, *Surface Sci.*, **60**(1977)528.
6. H. Frinet, P. Rouillon and B. Daulik, *J. Catalysis*, **61**(1980)553.
7. H. Siepter and H. Ibach, *Surface Sci.*, **77**(1978)109.
8. a. S. Sato and J. N. White, *J. Amer. Chem. Soc.*, **102**(1980)7206.
- b. S. Sato and J. N. White, *Ind. Eng. Chem. Prod. Res. Dev.*, **19**(1980)542.
- c. S. Sato and J. N. White, *Chem. Phys. Letters*, **70**(1980)131.
- d. S. Sato and J. N. White, *Chem. Phys. Letters*, **72**(1980)83.
- e. S. Sato and J. N. White, *J. Catalysis*, **60**(1981)128.
- f. S. Sato and J. N. White, *J. Phys. Chem.*, **85**(1981)592.
9. a. S. J. Tauster, S. C. Fung and R. L. Garten, *J. Amer. Chem. Soc.*, **100**(1978)170.
- b. S. J. Tauster, S. C. Fung, R. T. Baker and J. A. Horeley, *Science*, **211**(1981)1121.
10. a. M. A. Vannice and R. L. Garten, *J. Catalysis*, **56**(1979)236.
- b. M. A. Vannice and R. L. Garten, *J. Catalysis*, **66**(1980)242.
11. Katsumi Tanaka and J. N. White, *J. Phys. Chem.* (in press).
12. R. M. Hummer, S. A. Francis and R. P. Elchman, *Spectrochim. Acta*, **21**(1965)1295.
13. G. Blyholder, *J. Phys. Chem.*, **68**(1964)2772.
14. P. Hollins and J. Pritchard, "Vibrational Spectroscopies for Adsorbed Species", *ACS Symposium Series 137*(1980)51, A. T. Bell and M. L. Hair, ed.
15. D. Reinalda and V. Ponec, *Surface Sci.*, **91**(1979)113.
16. Katsumi Tanaka, K. L. Walters and R. P. Howe, *J. Catalysis*, **75**(1982)23.
17. J. C. Campuzano and R. G. Greenler, *Surface Sci.*, **81**(1979)301.
18. A. M. Bradshaw and P. M. Hoffmann, *Surface Sci.*, **72**(1978)513.
19. B.-H. Chen and J. N. White, *J. Phys. Chem.* (in press).
20. D. M. Collins, J. B. Lee and M. E. Spicer, *Surface Sci.*, **55**(1976)389.
21. G. Ertl, M. Neumann and K. M. Scholtz, *Surface Sci.*, **54**(1977)393.
22. D. R. Milne, J. Baret, C. A. Becker and L. Wharton, *Surface Sci.*, **100**(1981)263.
23. R. W. McCabe and L. D. Schmidt, *Surface Sci.*, **55**(1977)189.
24. C. T. Campbell, G. Ertl, H. Ibach and J. Sauer, *Surface*

- Sci., 107(1981)287.
25. D. M. Collins and W. E. Spicer, *Surface Sci.*, 60(1977)85.
26. M. R. McClellan, J. L. Gland and T. R. McFarley, *Surface Sci.*, 112(1981)63.
27. A. Sartak, J. Sarhany and A. Sittel, *J. Catalysis* 72(1981)236.
28. R. T. Baker, E. B. Prestidge and R. L. Garten, *J. Catalysis*, 50(1979)293.
29. L. Dubois and G. A. Samadaj, "Vibrational Spectroscopies for Adsorbed Species", ACS Symposium Series, 137(1980)166, A. T. Bell and M. T. Halicz, ed.
30. C. T. Campbell, G. Ertl, R. Kuipers and J. Segner, *Surface Sci.*, 107(1981)220.
31. a. J. T. Yates, Jr., T. M. Duncan, S. D. Worley and R. W. Vaughan, *J. Chem. Phys.*, 70(1979)1219.
b. B. J. C. Yates, L. L. Marrell and E. B. Prestidge, *J. Catalysis*, 57(1979)41.
- c. R. B. Cavanagh and J. T. Yates, Jr., *J. Chem. Phys.*, 74(1981)4150.
32. R. B. Cavanagh and J. T. Yates, Jr., *J. Catalysis* 68(1981)22.
33. T. M. Apple and C. Bytowski, *J. Catalysis* 71(1981)316.

Table 1. Experimental Conditions and Observed CO Band Frequencies.

Experimental Conditions	Observed Frequency (cm ⁻¹)
(1) 400-200-400 (Fig. 1)	
5 torr CO ads. 25°C	2185 2094 — 1854
Evacuation at 25°C	— 2078 — 1854
Evacuation at 80°C	— 2074 2063 —
Evacuation at 150°C	— — 2060 —
Evacuation at 200°C	— — — —
5 torr CO ads. 25°C	2185 2094 2080 1854
(2) 400-400-400 (Fig. 4)	
10 torr CO ads. 25°C	2185 2083 —
Evacuation at 25°C	— 2072 —
Evacuation at 150, 200°C	— — 2065 —
6 torr CO ads. 25°C	— 2075 —
(3) 400-40-400 (Fig. 5)	
0.8 torr CO 25°C 5 min.	2185 2097 — 1854 2130
0.8 torr CO 25°C 120 min.	2185 2097 — 1854 2130 1880
37 torr CO 25°C 150 min.	2185 2097 2077 1831 2120 1880
37 torr CO 25°C 63 hrs.	— 2084 2077 1854 2112 (1880) 2080, 1942
Evacuation at 25°C	— 2094 2072 1854 — — (1942)
Evacuation at 150°C	— — 2059 — — —
Evacuation at 200°C	— — — — —
5 torr CO 25°C 5 min.	2185 2086 2080 1854 2131 — —
(4) O ₂ 400-40-400 (Fig. 7)	
7 torr CO 25°C 7, 80 min.	2185 2086 — 1854 2130 —

(continued on next page)

Examination at 25°C -- 2002 2000 1854 2120 --
 Examination at 100°C -- -- -- 2005 -- 2131 -- 2101

Table 2. Assignment of CO bands.

Frequency/cm ⁻¹	Species	Site
2185	L ^(a)	TiO ₂
2130	L	Pt(O ₂)/Terraces
2101	L	Pt(O ₂)/Step
2094	L	Pt/Terraces
2077	L	Pt/Step
1860	B	Pairs of Pt(O ₂)
1854	B	Pairs of Pt
2060, 1942	T	Edge Pt

(a) L, B, and T denote linear, bridge and twin sites. Pt(O₂) denotes oxygen covered Pt.

FIGURE CAPTIONS

Figure 1. Spectra for CO adsorption on Fe/TiO_2 reduced at 200°C (400-200-400). (a) 5 torr CO. (b) Evacuation of (a) at 25°C . (c) Evacuation at 80°C . (d) Evacuation at 150°C . (e) Evacuation at 200°C . (f) 5 torr of CO after (e).

Figure 2. Adsorption of an equimolar mixture of C^{16}O and C^{18}O on Fe/TiO_2 (400-200-400). (a) 6 torr of mixture. (b)-(e) Evacuation of (a) at 25, 80, 150 and 200°C respectively.

Figure 3. Exchange of C^{18}O with preadsorbed C^{16}O on Fe/TiO_2 (400-200-400). (a) 8 torr C^{16}O . (b) Evacuation of (a) at 25°C . (c)-(e) Exposure of (b) to 3 torr C^{18}O for 5 min, 30 min and 18 hr, respectively. (f)-(g) Evacuation of (e) at 25 and 80°C , respectively.

Figure 4. CO adsorption on Fe/TiO_2 (400-400-400). (a) 10 torr CO. (b) Evacuation of (a) at 25°C . (c) 1 atm CO after (b). (d)-(f) Evacuation of (c) at 25, 150 and 200°C , respectively. (g) 6 torr CO after (f). (h) Evacuation of (g) at 25°C .

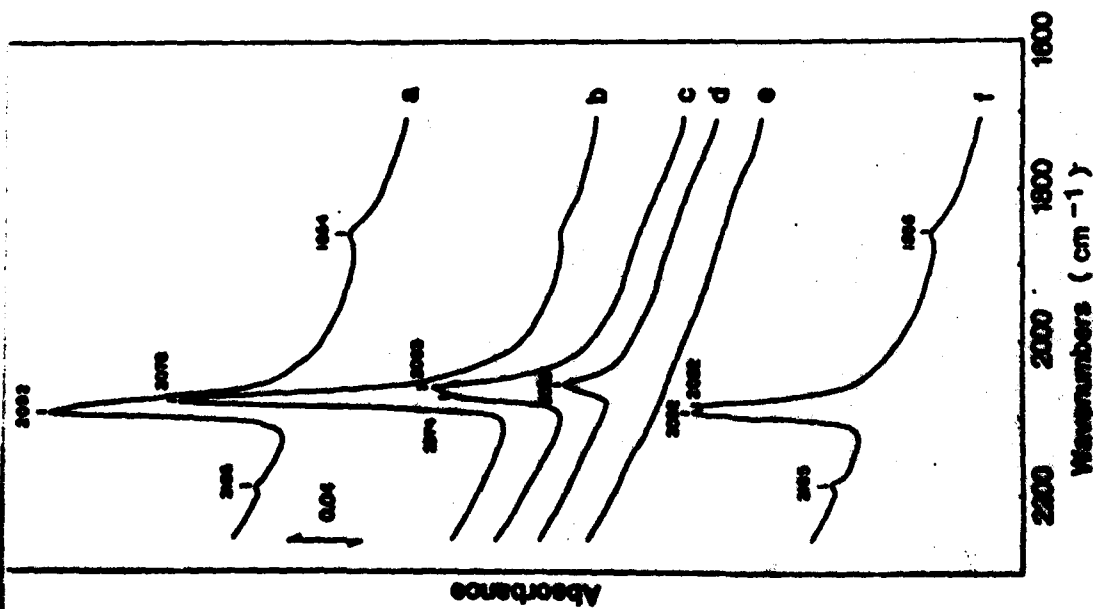
Figure 5. CO adsorption spectra on oxidized Fe/TiO_2 (600-80-400). CO pressure was increased from 0.8 to 37 torr after 120 min. Exposure times were: (a) 5 min, (b) 60 min, (c) 120 min, (d) 125 min, (e) 180 min, (f) 270 min, and (g) 48 hr. After (g) the system was evacuated at: (h) 25°C , (i) 80°C , (j) 150°C , and (k) 200°C . (l) 5 torr

CO after (k).

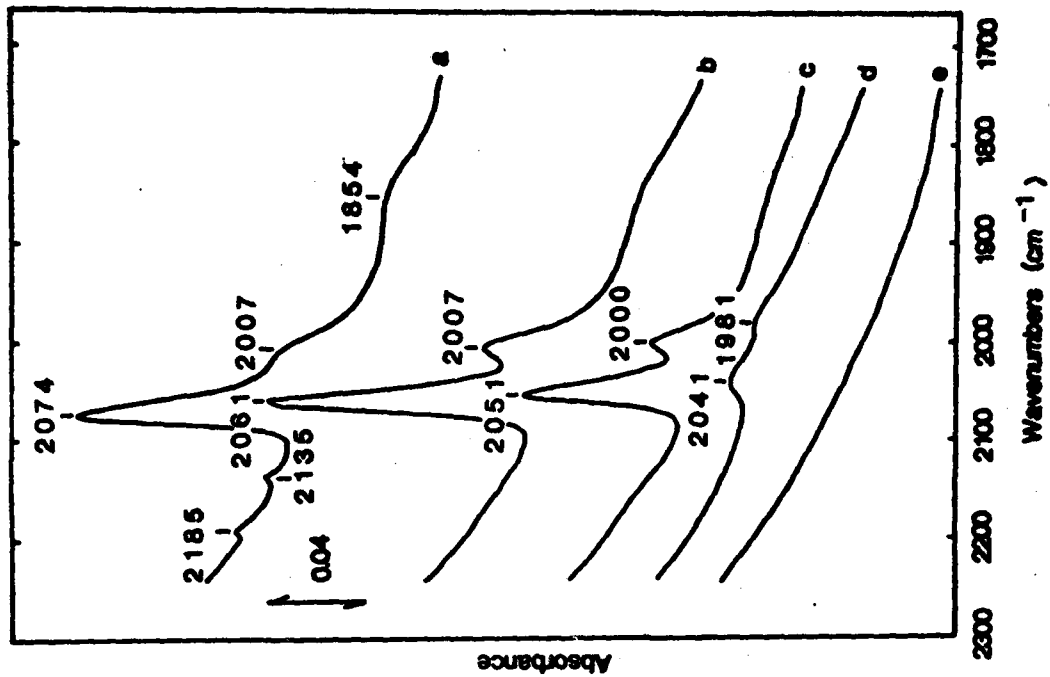
Figure 6. Time dependence of intensity changes for spectra of Fig. 5.

Figure 7. CO adsorption on an oxidized Fe/TiO_2 (400-80-400) reduced with O_2 at 25°C . Exposure of 7 torr CO for (a) 7 min and (b) 80 min. Evacuation of (b) at: (c) 25°C , (d) 100°C , and (e) 200°C .

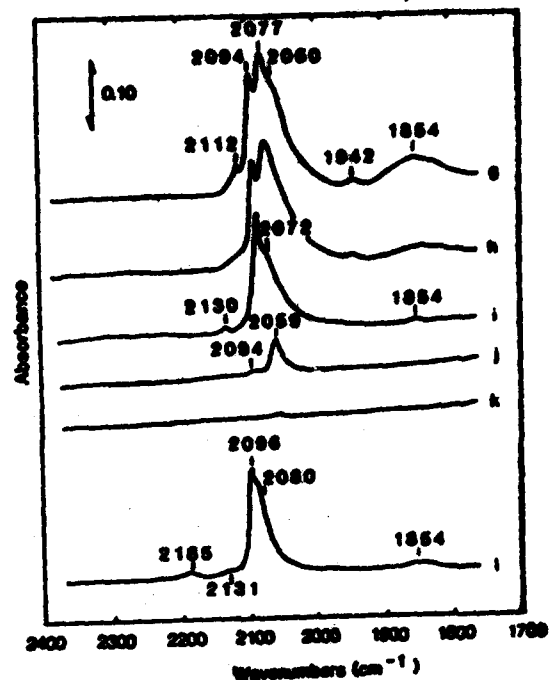
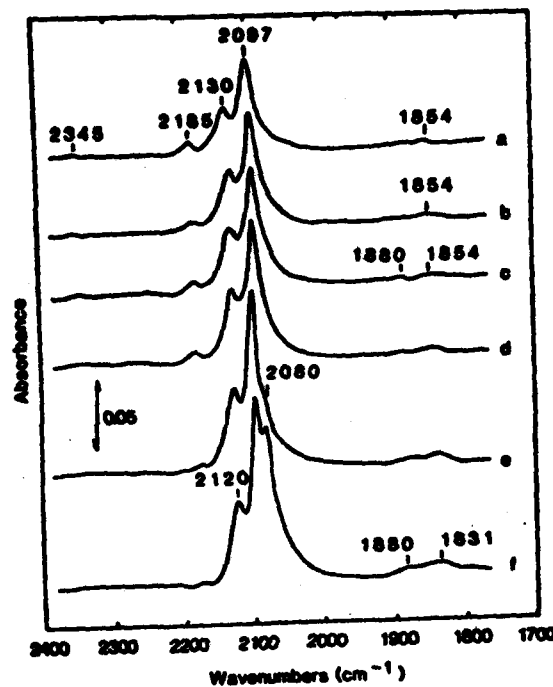
Figure 8. Effect of H_2 (1 atm) introduction on a Fe/TiO_2 sample preduced with CO.



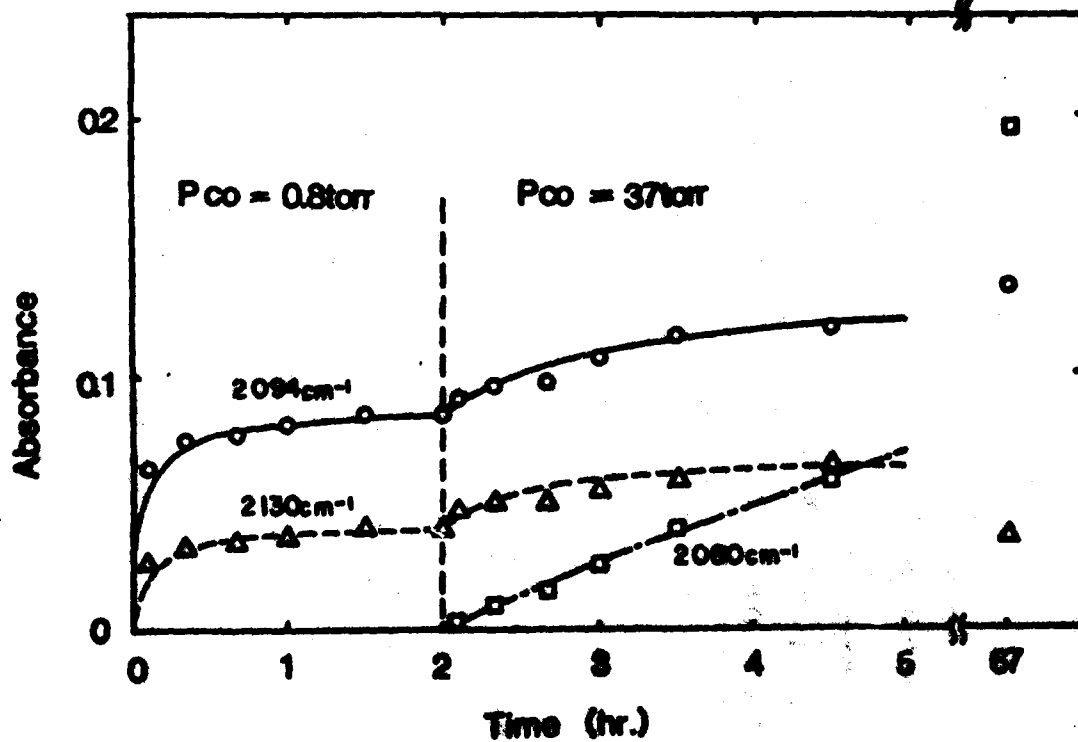
Trans-1,4-dichloro-2-butene, 70.1



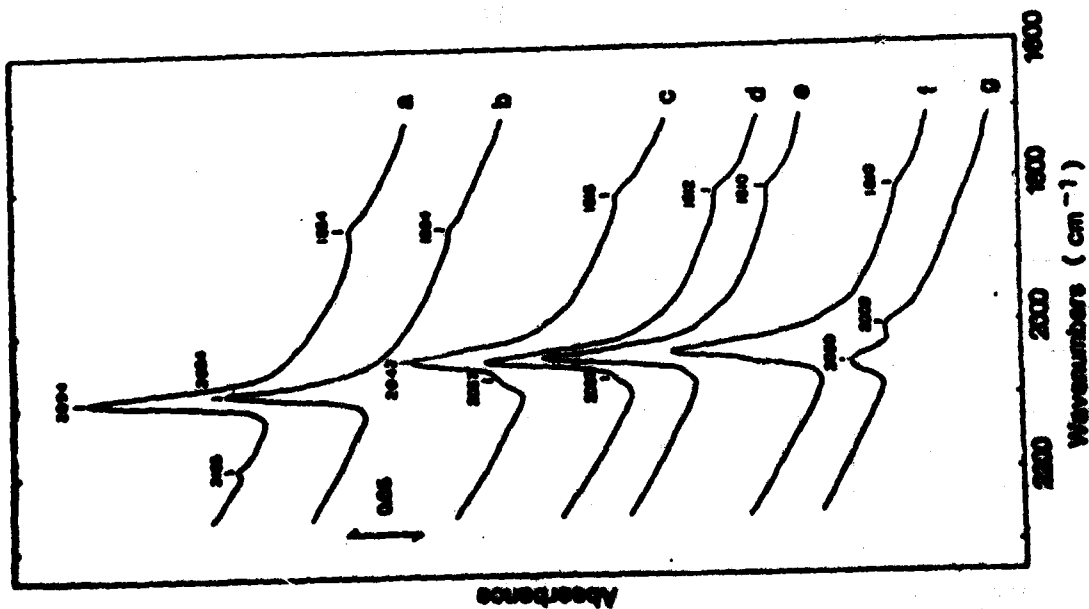
Trans-1,4-dichloro-2-butene, 70.2



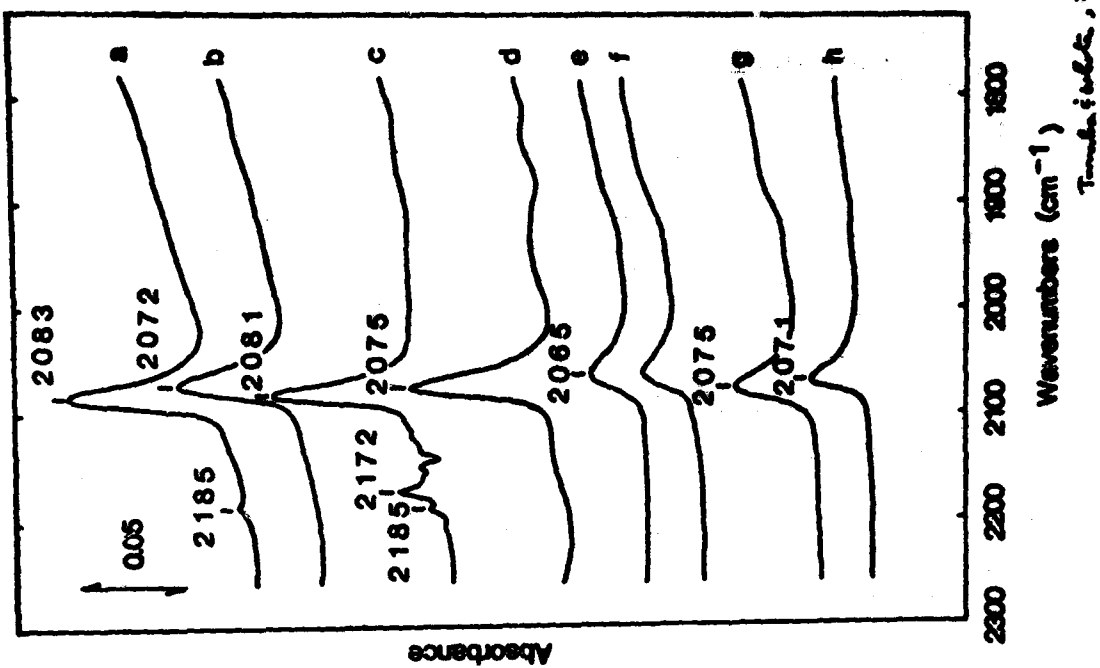
Tennant & White, 1955



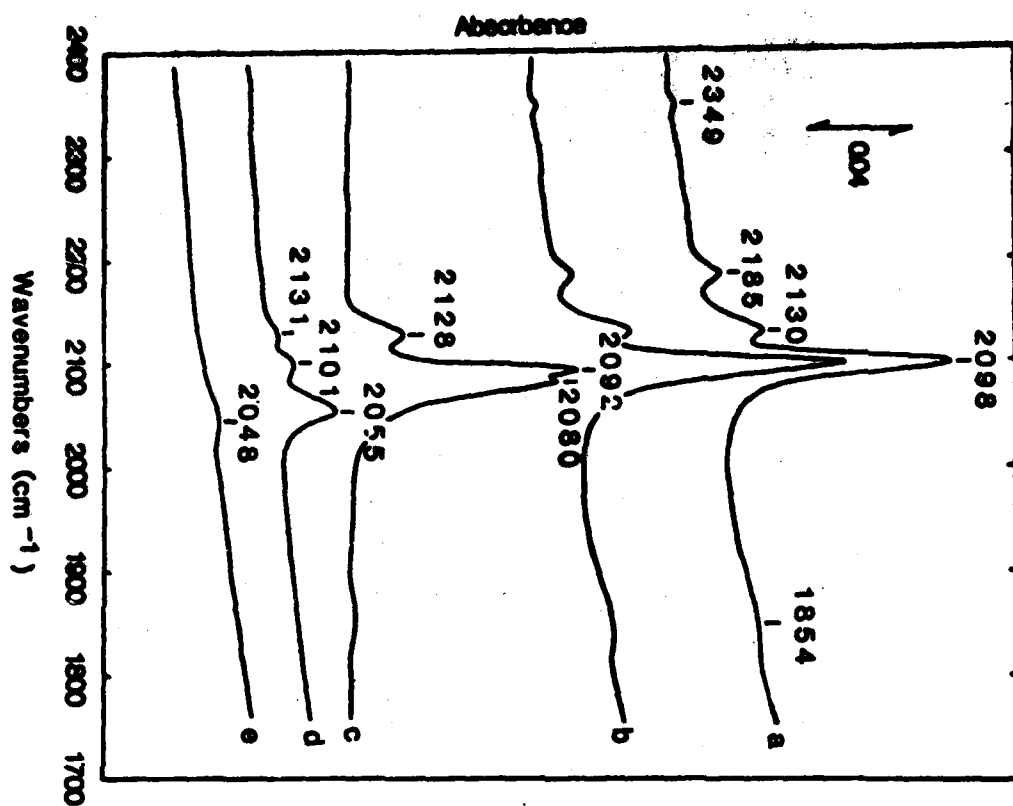
Tennant and White, 1955



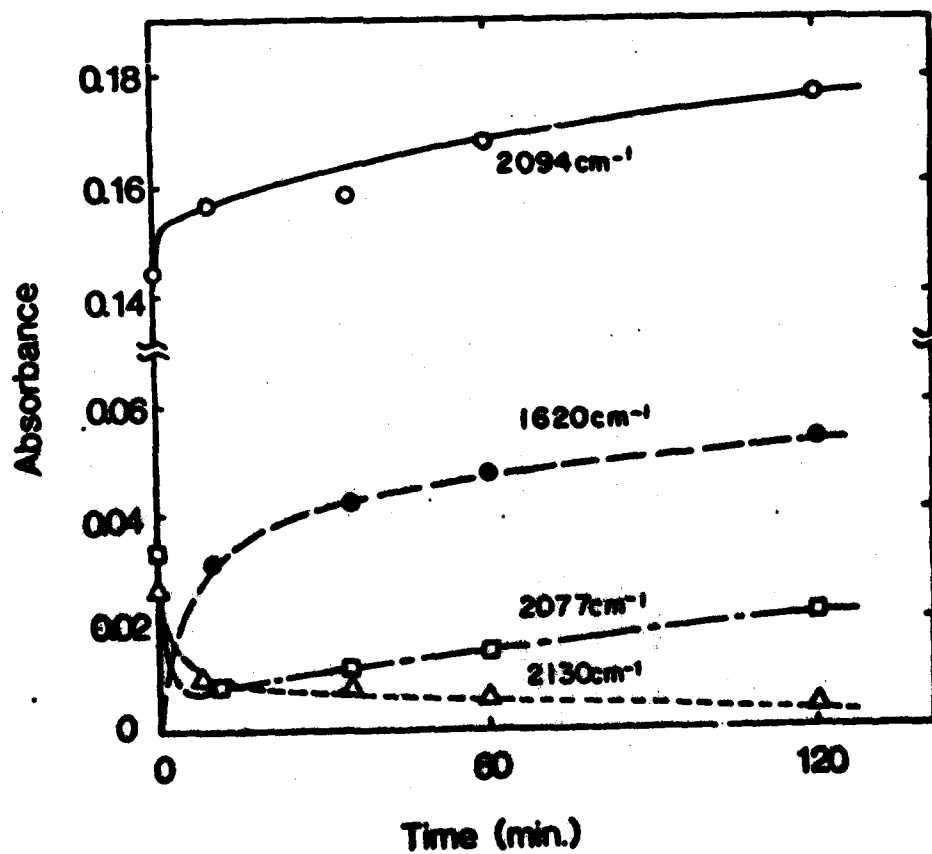
Trans-1,4,7,10-tetraene, 75-8



Trans-1,4,7,10-tetraene, 75-8



Reuter and Wicks, 1977



Reuter and Wicks, 1977

SP472-3/1A1

472(CAS):716:106
70-472-606

TECHNICAL REPORT DISTRIBUTION LIST, CON

No.
OfficeNo.
Office

Office of Naval Research
Attn: 472
800 North Quincy Street
Arlington, Virginia 22217

ONR Western Regional Office
Attn: Dr. E. J. Wrenn
1030 East Green Street
Anaheim, California 92806

ONR Eastern Regional Office
Attn: Dr. L. E. Perkins
Building 114, Section 8
646 Summer Street
Boston, Massachusetts 02210

Director, Naval Research Laboratory
Attn: Code 0100
Washington, D.C. 20390

The Assistant Secretary
of the Navy (NSAS)
Department of the Navy
Room 4736, Pentagon
Washington, D.C. 20350

Commander, Naval Air Systems Command
Attn: Code 310C (R. Macmillan)
Department of the Navy
Washington, D.C. 20360

Defense Technical Information Center
Building 5, Cameron Station
Alexandria, Virginia 22304

Dr. Fred Sealford
Chemistry Division, Code 0100
Naval Research Laboratory
Washington, D.C. 20375

Mr. James Bailey
JTRAC Code 2003
Annapolis, Maryland 21403

Dr. A. H. Ammons
Administrative Librarian
PLASMA/AMMUN
May 1968
Beverly, New Jersey 08004

U.S. Army Research Office
Attn: CDD-4A-1P
P.O. Box 1211
Research Triangle Park, N.C. 27709

Naval Ocean Systems Center
Attn: Mr. Joe McCartney
San Diego, California 92132

Naval Weapons Center
Attn: Dr. A. B. Amster,
Chemistry Division
China Lake, California 93555

Naval Civil Engineering Laboratory
Attn: Dr. R. W. Drish
Port Hueneme, California 93041

Department of Physics & Chemistry
Naval Postgraduate School
Monterey, California 93940

Scientific Advisor
Commandant of the Marine Corps
(Code 1D-1)
Washington, D.C. 20380

Naval Ship Research and Development
Center
Attn: Dr. G. Romajian, Applied
Chemistry Division
Annapolis, Maryland 21401

Naval Ordnance Systems Center
Attn: Dr. S. Yamasaki, Marine
Sciences Division
San Diego, California 92132

Mr. John Reple
Materials Branch
Naval Ship Engineering Center
Philadelphia, Pennsylvania 19112

SP472-3/1A7

TECHNICAL REPORT DISTRIBUTION LIST, 056

No.
OfficeNo.
Office

Dr. G. A. Somerjai
Department of Chemistry
University of California
Berkeley, California 94720

Dr. L. W. Jarvis
Surface Chemistry Division
5555 Overlook Avenue, S.W.
Washington, D.C. 20375

Dr. J. B. Hudson
Materials Division
Kansselaer Polytechnic Institute
Troy, New York 12181

Dr. John T. Yates
Surface Chemistry Section
National Bureau of Standards
Department of Commerce
Washington, D.C. 20234

Dr. Theodore E. Nadey
Surface Chemistry Section
Department of Commerce
National Bureau of Standards
Washington, D.C. 20234

Dr. J. N. Chifed
Department of Chemistry
University of Texas
Austin, Texas 78712

Dr. Keith H. Johnson
Department of Metallurgy and Materials
Science
Massachusetts Institute of Technology
Cambridge, Massachusetts 02139

Dr. J. E. Demuth
IBM Corporation
Thomas J. Watson Research Center
P.O. Box 218
Yorktown Heights, New York 10594

Dr. C. P. Flynn
Department of Physics
University of Illinois
Urbana, Illinois 61801

Dr. W. Kohn
Department of Physics
University of California
(San Diego)
LaJolla, California 92037

Dr. R. L. Park
Director, Center of
Materials Research
University of Maryland
College Park, Maryland 20742

Dr. W. T. Paris
Electrical Engineering
Department
University of Minnesota
Minneapolis, Minnesota 55455

Dr. Chia-wei Yoo
Department of Physics
Northwestern University
Evanston, Illinois 60201

Dr. D. C. Naitis
Polytechnic Institute of
New York
333 Jay Street
Brooklyn, New York 11201

Dr. Robert N. Hunter
Department of Chemistry
University of Minnesota
Minneapolis, Minnesota 55455

Dr. E. P. Van Dyne
Chemistry Department
Northwestern University
Evanston, Illinois 60201

UNION BOND DISTRIBUTION LIST, 1966



Dr. J. Edgar
Department of Chemistry
New York Institute
of Technology
400 5th Avenue
Brooklyn, Illinois 60022

Dr. H. G. Lippert
Department of Mathematics
and Mining Engineering
University of Minnesota
Duluth, Minnesota 55812

[illegible]

Dr. Robert C. Brown
Department of Chemistry
The French Institute
3301 Ellis Avenue
Chicago, Illinois 60637

Dr. E. S. Ellis
Department of Zoology
University of California,
Irvine, California 92697

B. S. Graham
Courtesy, New York
George Washington University
Washington, D.C.

**Dr. J. Peter
Chemistry Department
University of California,
Santa Barbara**

THE UNIVERSITY OF CHICAGO

二、

1990



Dr. Martin Fleischmann
Department of Chemistry
Southampton University
Southampton SO9 5NH
Hampshire, England

Dr. J. Otto Young
Chemistry Department
State University of New
York at Buffalo
Buffalo, New York 14216

Dr. G. Rubloff
I.B.M.
Thomas J. Watson Research Center
P. O. Box 218
Yorktown Heights, New York 10598

Dr. J. A. Gardner
Department of Physics
Oregon State University
Corvallis, Oregon 97331

Dr. G. B. Stala
Mechanical Engineering Department
Northwestern University
Evanston, Illinois 60201

Dr. E. G. Speers
Chemistry Department
Northwestern University
Evanston, Illinois 60201

Dr. R. V. Plesner
University of Pennsylvania
Department of Physics
Philadelphia, Pennsylvania 19106

Dr. E. Meyer
Department of Chemistry
Case Western Reserve University
Cleveland, Ohio 44106

THE
JOURNAL
OF
THE
ROYAL
ANTHROPOLOGICAL
INSTITUTE
OF GREAT BRITAIN
AND IRELAND
PART I
1901

TECHNICAL BOOK DISTRIBUTION LTD. 666

2000

Professor H. Vinograd
The Pennsylvania State University
Department of Chemistry
University Park, Pennsylvania 16802

Professor T. F. George
The University of Rochester
Chemistry Department
Rochester, New York 14627

Professor Dudley R. Harruckeck
Harvard College
Office for Research Contracts
1380 Massachusetts Avenue

Professor Maria Metiu
University of California,
Santa Barbara

Professor A. Steckl
Rensselaer Polytechnic Institute
Santa Barbara, California 93106

**System Engineering
Integrated Circuits Laboratories
Troy, New York 12181**

Professor A. G. Michel
University of Massachusetts
Chemistry Department
Amherst, Massachusetts 01003

Dr. A. C. Foster
Huguenot Research Laboratories
3011 Malibu Canyon Road
Malibu, California 90265

Dr. Stephen Webber
Dept. of Chemistry
University of Toronto